Journal of Optoelectronics and Advanced Materials Vol. 7, No. 6, December 2005, p. 3169 - 3177

STRUCTURE AND TEXTURE OF SOME KEGGIN TYPE HETEROPOLYACIDS SUPPORTED ON SILICA AND TITANIA

A. Popa*, V. Sasca, E. E. Kiš[a], Radmila Marinković-Nedučin[a], M. T. Bokorov[b], J. Halasz[c]

Institute of Chemistry Timişoara, Bl. Mihai Viteazul 24, Romania
[a]University of Novi Sad, Faculty of Technology, Cara Lazara 1, Novi Sad, Serbia and Montenegro
[b]University Centre For Electron Microscopy, University of Novi Sad, Dositeja Obradovica 2, Serbia and Montenegro
[c]University of Szeged, Dept. of Applied and Environmental Chemistry, Rerrich ter 1, H-6720 Szeged, Hungary

The structure and texture of $H_3PMo_{12}O_{40}$ (HPMo) and $H_4PVMo_{11}O_{40}$ (HPVMo) supported on silica (Aerosil- Degussa and Romsil types) and titania are studied by XRD, FT-IR, low temperature nitrogen adsorption and scanning electron microscopy. All supported heteropolyacids (HPAs) were prepared by impregnation using the incipient wetness techniques with a mixture water: ethanol = 1:1. In order to obtain highly dispersed HPAs species, the samples were prepared with different quantities of active compounds: 5-40 wt. %. The effect of loading on textural and structural properties was examines for supported HPAs catalysts comparatively with parent acids and their mechanical mixtures. It is found that most of HPMo and HPVMo (active phases) in samples are well dispersed on the support and both silica and titania supported HPAs still keeps its Keggin structure. The surface morphology of the silica and titania supported samples is almost similar to that of support, and thereby a relatively uniform distribution of active phase in the support pores are expected. The dispersion of active phase on support was estimated from XRD pattern, and it decreases with acid content. FTIR spectra of mechanical mixtures of HPA with silica are similar to the supported samples, so this method cannot distinguish these materials. Contrasting with supported HPAs on silica, their mechanical mixtures exhibit sharp and narrower diffraction lines, more similar to crystalline pure HPAs.

(Received October 3, 2005; accepted November 24, 2005)

Keywords: Heteropolyacids, Silica, Titania, Texture, Structure, BET, XRD

1. Introduction

Keggin type heteropolyacids (HPAs) have been widely used in acid-catalysed reactions as well as oxidation reactions both in the heterogeneous and homogeneous systems [1-7]. Heteropolyacids have been pointed out lately as versatile green catalysts for a variety of reactions: alkylation and acylation of aromatics, esterification, liquid bi-phase processes [8-9]. There is an interest to substitute liquid catalysts (e.g. H_2SO_4, HF, p-toluenesulphonic acid) – which are corrosive, toxic and difficult to separate from reaction solution- by more environmentally friendly solid acids. Among many possible forms of heteropolyacids used as catalysts, there are their salts and supported heteropolyanions [10-18].

Pure HPAs generally show low catalytic reactivity owing to their small surface area. In order to be more effective for catalytic reactions, HPAs are usually impregnated on different porous materials. The type of carrier, textural and structural properties influence the thermal stability and the catalytic activity of Keggin-type heteropolyacids.

* Corresponding author: sandu@acad-icht.tm.edu.ro

In order to obtain highly dispersed heteropolyacids species, $H_3PMo_{12}O_{40}$ and $H_4PVMo_{11}O_{40}$ were supported on various supports: silica (Aerosil- Degussa and Romsil types) and titania. The goal of this work was to characterise the texture and structure of these heteropolyacids supported on silica and titania in reference to the bulk solid acids and their mechanical mixtures.

2. Experimental

H_4 $[PMo_{11}VO_{40}]\cdot 12H_2O$ was prepared by two methods: Tsigdinos and hydrothermal method. $H_3[PMo_{12}O_{40}]\cdot 13H_2O$ was purchased from Merck. The as-received material was recrystallized prior to use. In the present work three types of supports were used: silica (Aerosil- Degussa and Romsil types) and TiO_2. HPMo and HPVMo heteropolyacids were deposited by impregnation in the amount varying from 10 to 40 % loading (denoted for example $30HPMo/SiO_2$), depending of support type.

Textural characteristics of the outgassed samples were obtained from nitrogen physisorption using a Micrometrics ASAP 2000 instrument. The specific surface area S_{BET}, mean cylindrical pore diameters d_p and adsorption pore volume V_{pN2} were determined. Prior to the measurements the samples were degassed to 10^{-5}Pa at 150 ºC. The BET specific surface area was calculated by using the standard Brunauer, Emmett and Teller method on the basis of the adsorption data. The pore size distributions were calculated applying the Barrett-Joyner-Halenda (BJH) method to the desorption branches of the isotherms. The IUPAC classification of pores and isotherms were used in this study.

Microstructure characterisation of the catalyst particles was carried out with a JEOL JSM 6460 LV instrument equipped with an OXFORD INSTRUMENTS EDS analyser. Powder materials were deposited on adhesive tape fixed to specimen tabs and then ion sputter coated with gold.

Powder X-ray diffraction data were obtained with a XR Fischer diffractometer using the Cu K_α radiation in the range $2\theta = 5 \div 60°$.

The IR absorption spectra were recorded with a Biorad FTS 60A spectrometer (spectral range 4000-200 cm^{-1} range, 256 scans, and resolution 2 cm^{-1}) using KBr pellets.

3. Results and discussion

The nitrogen adsorption isotherms of heteropolyacids supported on Romsil, Aerosil and titania are shown in Figs. 1a, 2a and 3a. For 30HPVMo/Romsil we observe a type IV isotherm with a type H1 hysteresis loop in the high range of relative pressure. For the values of relative pressure higher than 0.8 condensation take place giving a sharp adsorption volume increase. This behavior indicates that this sample has a mesoporous character. Hysteresis loop type shows that HPVMo/Romsil sample consists of agglomerates or compacts of approximately uniform spheres in fairly regular array. Both HPMo and HPVMo heteropolyacids supported on Romsil present the type IV isotherm with a type H1 hysteresis loop.

The adsorption-desorption isotherms of nitrogen for HPMo and HPVMo supported on Aerosil, present also type-IV isotherm with a type H1 hysteresis loop in the 0.85-1 range of relative pressure (Fig. 2a). The shape of desorption branch of isotherms for Aerosil supported samples is a little different then Romsil supported ones.

For titania supported HPAs the adsorption-desorption isotherms show a type H3 hysteresis loop in the middle range of P/P_0 characteristic for aggregates of plate-like particles forming slit-shaped pores (Fig. 3a).

The pore size distributions were calculated by Barret-Joyner-Halenda (BJH) method applied to the desorption branches of the isotherms. BJH method is further used to check and to complete the previous results. The pore size distribution curve of 30HPVMo supported on Romsil and Aerosil show a maximum at 25-26 nm (Fig. 1b, 2b). Pores with sizes belonging to the entire range characteristic for mesoporosity (2-50 nm) and little macroporosity appear for HPAs supported on both types of silica at loading varying from 10 wt.% to 30 wt.%. The shape of pore size distribution curves of HPAs/Romsil is broad and asymmetric, the size of pores being from 10 nm to 80 nm. The pore size distribution curves of HPAs/Romsil are broader then HPAs/Aerosil ones, especially in the macroporosity range, showing a nonuniformity of the porous structure. The pore size distribution

curves of both HPAs supported on titania are completely different showing two maximums at 1.64 nm (microporosity range) and 3.56 nm (mesoporosity range).

The specific surface areas of used supports are 90 m^2/g for silica-Romsil, 235 m^2/g for silica-Aerosil and 325 m^2/g for titania [17]. The specific surface areas of HPAs deposited on all supports decreased with active phase concentration (Table 1). Thus, the specific surface area of silica Aerosil supported heteropolyacids decreased from 235 m^2/g for Aerosil support to 140.7 m^2/g for 20HPMo/Aerosil sample, respectively to 153 m^2/g for the 20 HPVMo/Aerosil sample. In addition, the specific surface area decreased drastically from 325 m^2/g (TiO_2 support) to 248.4 m^2/g for 20 HPVMo/TiO_2 and to 115.9 m^2/g for 40 HPVMo/TiO_2, respectively.

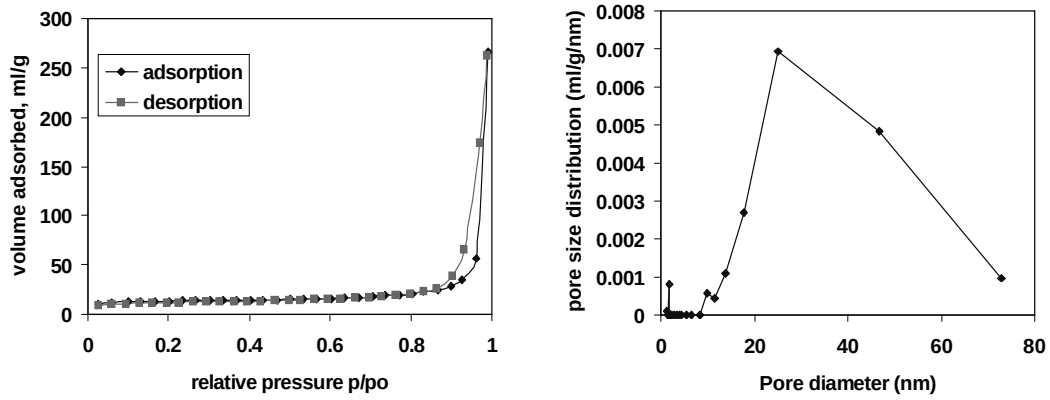

Fig. 1. Nitrogen adsorption-desorption isotherms at 77 K (a) and pore size distribution derived from the desorption branch of nitrogen physisorption (b) of 30 HPVMo supported on Romsil.

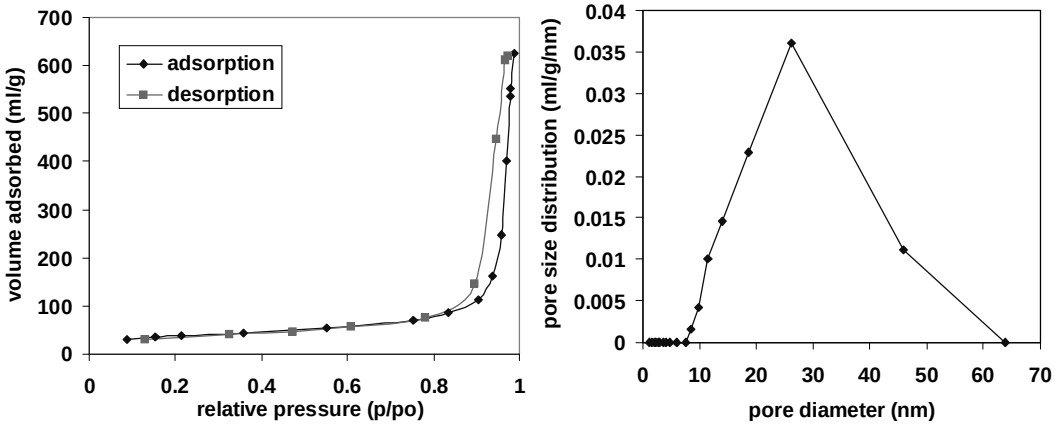

Fig. 2. Nitrogen adsorption-desorption isotherms at 77 K (a) and pore size distribution derived from the desorption branch of nitrogen physisorption (b) of 30HPVM supported on Aerosil.

Specific surface area diminishing could be explained owing to support pores blocking by active phase, as well as by the formation of some HPAs crystallites agglomeration (especially at high loading of active phase). As a large percentage of pores of titania supported HPAs are micropores (below 2 nm) and the Keggin unit diameter is ~ 12 Å, it stand to reason that micropores are blocked by active phase and the specific surface area drops drastically by increasing the active phase loading.

The mean pore diameter varies in the range 2.8-26 nm for Romsil supported HPAs, 20-28 nm for Aerosil supported HPAs and 1.2-4.7 nm for titania supported HPAs in function of different surface coverage, as it results from the pores size distribution curves. For all loadings, both HPAs

exhibit differential pore size distribution in the mesoporosity range and with only little macroporosity for silica supported samples, and pore size distribution in the microporosity and mesoporosity range for titania supported samples.

In order to confirm the presence of the Keggin anion on silica and titania respectively, the supported HPAs samples were analysed by FTIR. The $PMo_{12}O_{40}^{3-}$ Keggin ion structure consists of a PO_4 tetrahedron surround by four Mo_3O_{13} formed by edge-sharing octahedra. These groups are connected each other by corner-sharing oxygen. This structure give rise to four types of oxygen, being responsible for the fingerprints bands of Keggin ion between 1200 and 700 cm^{-1}.

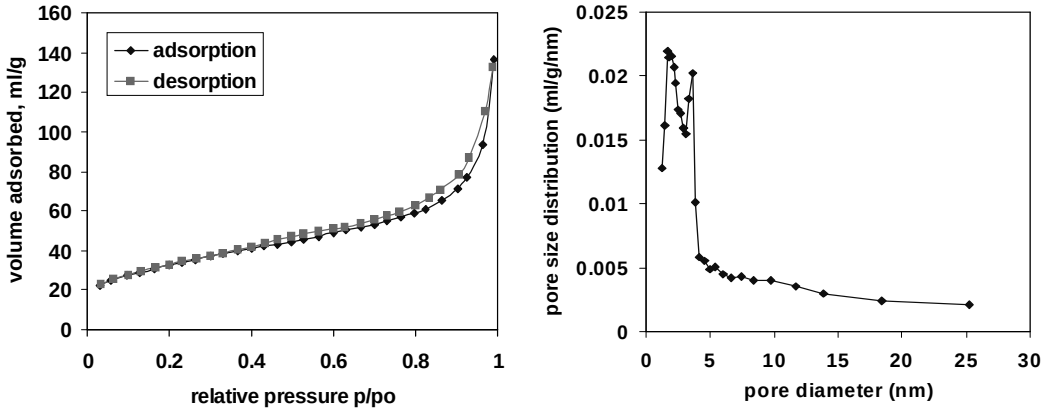

Fig. 3. Nitrogen adsorption-desorption isotherms at 77 K (a) and pore size distribution derived from the desorption branch of nitrogen physisorption (b) of 40HPVMo supported on titania.

The pure HPAs show an IR spectrum with the specific lines of the Keggin structure containing the main absorption lines at 1064 cm^{-1}, 960 cm^{-1}-965 cm^{-1}, 864 cm^{-1}-868 cm^{-1}, 784 cm^{-1} - 804 cm^{-1} assigned to the stretching vibrations ν_{as} P -O, ν_{as} Mo=O_t, ν_{as} Mo-O_c-Mo and ν_{as} Mo-Oe-Mo [9, 10]. These bands are maintained on the supported samples, but they are broadened and partially obscured because of the strong absorption bands of silica (1100, 800 and 470 cm^{-1}) (Fig. 4). The replacing of a Mo atom with a V atom leads to the appearance of two "shoulders" corresponding to the absorption maxim of the vibration ν_{as} (P-O_p) at 1080 cm^{-1} and ν_{as} (V-O_T) at 980 cm^{-1}. This confirms the presence of V^{5+} inside the MO_6 octahedra. These shoulders could not be seen in the IR spectra of supported HPAs as adsorption bands of silica overlap them completely [18].

On the other hand, FTIR spectra of mechanical mixtures of HPAs (HPMo, HPVMo) and silica (Romsil, Aerosil) or titania on the same loading range have shown similar characteristics with supported samples. Thus, FTIR method cannot distinguish unequivocally between supported HPAs and mechanical mixtures with silica and titania, respectively.

XRD patterns of various Romsil silica-supported HPMo and HPVMo samples with different loading are illustrated in Fig. 4 and 5, respectively. XRD patterns were obtained in order to be sure HPMo and HPVMo were effectively supported on silica, and to evaluate the dispersion state of the acid on support. Amorphous silica gel display only a broad band centred at $2\theta = 22^o$. It may be observed that some of the diffraction peaks characteristic of crystalline HPAs appeared on the supported catalysts. For samples with 10 wt.% loading, XRD has shown larger peak at $2\theta = 22^o$ attributed to silica, but typical peaks of pure HPAs were not observed. For samples with 20 wt.% HPVMo loading, two very weak diffraction peaks characteristic of active phase can be seen around $2\theta = 7.8^o$ and 8.7^o, while in the case of 20HPMo/Romsil one weak peak are observed at $2\theta = 7.8^o$. The peaks become not only more evident on intensity, but also less broad (in comparison with pure HPAs pattern) as the concentration of active phase increases.

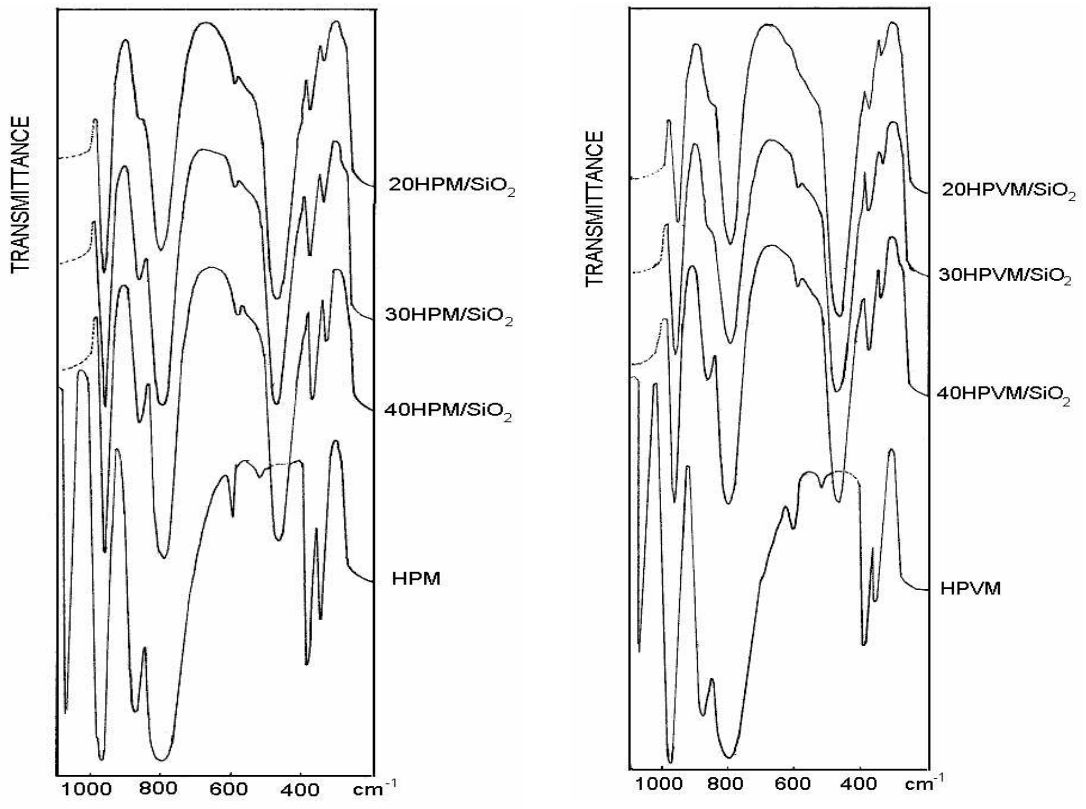

Fig. 4. IR Spectra of samples: HPMo and HPVMo supported on SiO_2 at different concentrations of the active phase.

Contrasting with supported HPAs on Romsil silica, mechanical mixtures of the acid with SiO_2 exhibit sharper and narrower diffraction lines more similar to crystalline HPMo and HPVMo, respectively. In order to make this comparison, XRD of the 30 wt.% HPMo and 30 wt.% HPVMo supported on Romsil and their mechanical mixtures with identical mass of HPAs were obtained. The results displayed on Fig. 4 and 5 show that the diffraction lines produced by mechanical mixtures resemble the pure crystalline HPMo and HPVMo. The characteristic reflections of HPMo and HPVMo present higher intensities and are less broad than those of the supported samples. XRD for supported HPAs is distinctive of mechanical mixtures of these solids, and, therefore, can be used to characterise these catalysts.

In order to estimate the dispersion of the active phase on silica support, the mean crystallite size has been calculated by Scherrer's equation [9] from the XRD patterns of the catalysts:

$$s_m = \frac{0.9\lambda}{B\cos\theta_B} \tag{1}$$

where s_m is the average particle size, B is the full width at half maximum (in 2θ) and θ_B is the Bragg angle.

Table 1. Characteristic parameters of the texture of pure and supported HPAo samples.

Sample	Surface area (m^2/g)	Pore volume, V_{IP} (cm^3/g)	Pore diameter, d_m (nm)
HPMo	3.53	0.011	14.08
HPVMo	3.89	0.012	12.66
10HPMo/Romsil	75.0	0.40	2.76
20HPMo/Romsil	66.9	0.36	11.1
30HPMo/Romsil	63.2	0.38	25.1
10HPVMo/Romsil	78.4	0.12	3.77
20HPVMo/Romsil	64.9	0.57	25.9
30HPVMo/Romsil	62.9	0.41	25.4
20HPMo/Aerosil	140.7	0.98	27.9
30HPMo/Aerosil	132.5	0.83	25.0
40HPMo/Aerosil	103.8	0.67	25.7
20HPVMo/Aerosil	153.0	0.86	22.7
30HPVMo/Aerosil	139.8	0.78	21.8
40HPVMo/Aerosil	112.1	0.62	20.4
20HPMo/TiO_2	240.2	0.28	4.66
30HPMo/TiO_2	165.8	0.22	4.12
40HPMo/TiO_2	85.8	0.14	1.23
20HPVMo/TiO_2	248.4	0.29	4.51
30HPVMo/TiO_2	182.4	0.24	3.91
40HPVMo/TiO_2	115.9	0.21	1.64

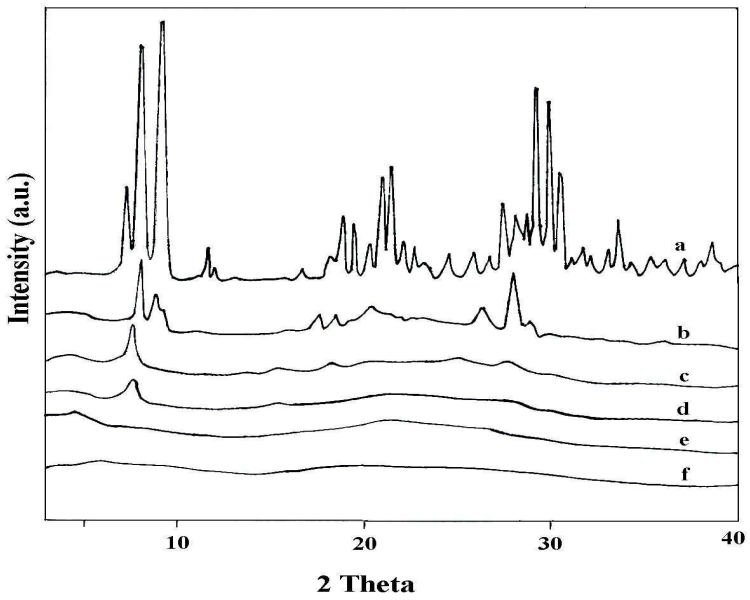

Fig. 5. XRD patterns of: a) $H_3PMo_{12}O_{40}$; b) 30 wt.% HPMo + SiO_2 mechanical mixture; c) 30 HPMo/SiO_2; d) 20 HPMo/SiO_2; e) 10 HPMo/SiO_2; f) SiO_2-Romsil.

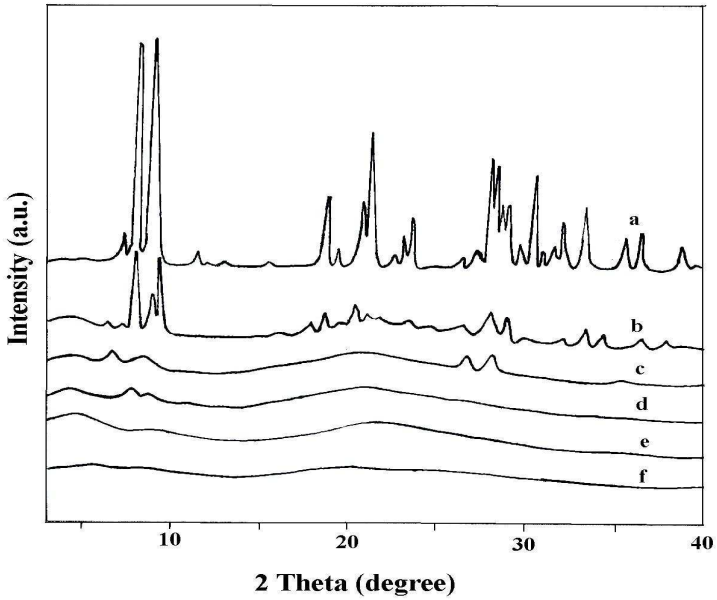

Fig. 6. XRD patterns of: a) $H_4PVMo_{11}O_{40}$; b) 30 wt.% HPVMo + SiO_2 mechanical mixture; c) 30 HPVMo/SiO_2; d) 20 HPVMo/SiO_2; e) 10 HPVMo/SiO_2; f) SiO_2-Romsil.

The equation was applied to each sample using $2\theta = 7.8^o$, which is less influenced by the diffracted broad band of non-crystalline silica. The mean diameters of the HPMo crystallites were 14.1, 15.6, 17.7 nm for the supported HPMo/silica with 10, 20, 30 wt.% acid loading and 26.5 nm for 30HPMo+silica mechanical mixture. In the case of HPVMo, the mean diameters of crystallites were 12.9, 14.0, 17.7 nm for the supported HPVMo/SiO_2 with 10, 20, 30 wt.% acid loading and 22.1 nm for 30HPVMo+silica mechanical mixture.

By using the same Scherrer equation, the main diameter of HPMo and HPVMo was 32 nm; therefore, higher dispersion of heteropolyacids clusters is achieved on supported catalysts. These data indicate a decrease of HPMo and HPVMo dispersion when increasing acid loading, which is expected based on formation of larger agglomerates on silica surface with concentration of acid impregnated on the support.

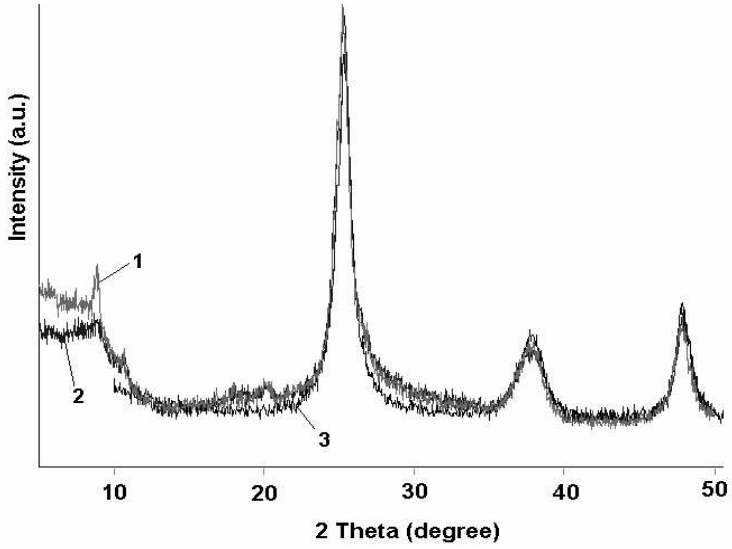

Fig. 7. X-ray diffraction patterns of titania supported HPAs: HPMo/TiO_2 (1), HPVMo/TiO_2 (2) and TiO_2 (3).

XRD patterns of titania-supported HPAs are shown in Fig. 7. The patterns of both HPAs/TiO_2, which were recorded after drying at 120ºC, shows the main peaks characteristic of titania support, and only at small angles (5-10º) some weak peaks corresponding to heteropolyacids could be observed. Therefore, the XRD data indicate that for amount of HPAs corresponding to theoretical monolayer, small quantities of HPAs crystallites are observed for titania-supported HPAs. So, at relatively high concentration of active phase (40% wt%) some HPAs molecules could not access to the support mesopores and crystallize as separate phases.

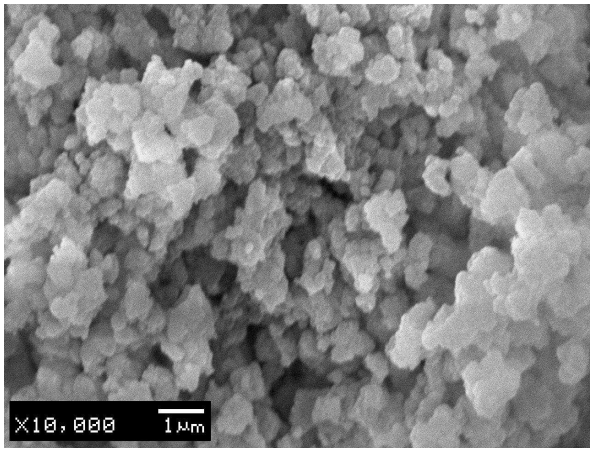

Fig. 8. SEM micrografs of 30HPVMo/Romsil.

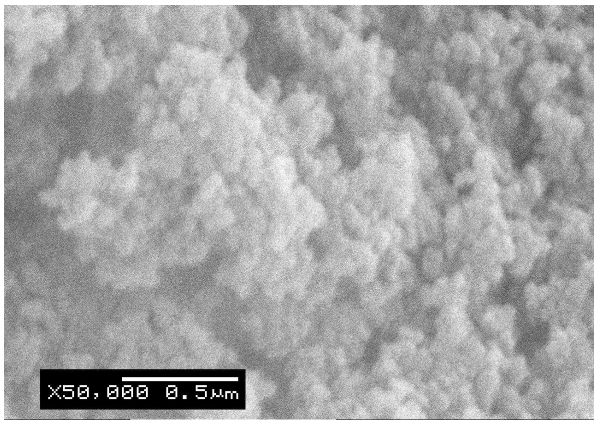

Fig. 9. SEM micrografs of 30HPVMo/Aerosil.

Silica Romsil support is composed of agglomerates of spherical particles with an average diameter below 1 μm (Fig. 8). The surface morphology of silica Romsil-supported HPAs is practically identical to that of the pure silica. From SEM images one can see that no separate crystallites of the bulk phase of HPAs were found in the supported samples. The micrographs of Aerosil supported HPAs show that they are agglomerates formed of small spherical particles 20-40 nm in diameter (Fig. 9). The surface of the titania supported HPAs is composed of agglomerates of irregular shape particles with diameter of 100-200 nm.

HPAs distribution on supported samples surface was analysed by EDS method, which was performed as point analysis on thin particles. By this technique were obtained the chemical composition of Mo and V elements. The EDS point analysis was made over several domains with 20×20 μm dimensions on the same sample. The analysis was repeated on different samples in order to ensure the reproducibility of the obtained results.

The pure HPAs were fully homogeneous and of exactly Mo:P:V composition as expected [16]. The silica and titania supported samples exhibit a constant distribution of molybdenum content and close to the stoichiometric value. The vanadium content of supported HPAs are quite difficult to

analyse because the V maximum is partially overlaped by Si or Ti maximum. Anyway, for supported samples one can observe the same behaviour like for unsupported HPAs, namely a relatively homogeneous distribution of molybdenum.

4. Conclusions

Different HPAs loading has a strong impact on the texture and structure of silica and titania supported 12-molybdophosphoric and 1-vanado 11-molybdophosphoric acids. As indicated by FTIR and XRD results, silica-supported and titania-supported HPAs still keeps its Keggin structure. For all loading, both HPAs exhibit differential pore size distribution in the mesoporosity range and with only little macroporosity for silica supported samples, and pore size distribution in the microporosity and mesoporosity range for titania supported samples.

The higher dispersion of HPMo and HPVMo is confirmed by the size of crystallites supported on silica determined by XRD. In addition, XRD patterns can differentiate supported samples from mechanical mixtures of heteropolyacids and silica, which cannot be evidenced by FTIR. A relatively uniform distribution of HPAs on the support surface is observed for all compositions of active phase. No separate crystallites of the bulk phase of HPAs were found in the SEM images of supported samples. According to EDS results the active phase is homogeneously distributed in the silica and titania matrix

Acknowledgment

These investigations were partially financed by the Ministry of Education and Research of Romania Grant No 32826/2004 and Ministry of Science and Environment Protection of the Republic of Serbia – Project 1368.

References

[1] N. Mizuno, M.Misono, Chem. Rev. **98,** 199 (1998).
[2] M. Misono, Catal.Rev.-Sci. Eng. **29,** 269 (1987).
[3] M. Misono, in Proc.10th Int. Congr. Catal., Budapest, L. Guczi (Eds), Elsevier, Amsterdam 1993, p. 69.
[4] F. Cavani, Catal. Today **41,** 73 (1998).
[5] E. Cadot, C. Marshal, M. Fournier, A. Teze, G. Herve, in Polyoxometalates, M. T. Pope and A. Muller (eds), Kluwer Acad. Publish., Dordrecht 1994, p. 315.
[6] S. Kastelan, E. Payen, J. B. Moffat, J. Catal. **125**, 45 (1990).
[7] S. Damyanova, J. L. G. Fierro, Chem. Mater. **10**(3), 871 (1998).
[8] M. Misono, T. Inui, Catal. Today **51,** 369 (1999).
[9] Y. Ono in Perspectives in Catalysis, J. M. Thomas, K. I. Zamaraev (eds), London.1992, p. 341.
[10] K. Brückman, M. Che, J. Haber, J. M. Tatibouët, Catal. Lett. **25**, 225 (1994).
[11] C. Trolliet, G. Coudurier, J. C. Vedrine, Topics in Catal. **15**(1), 73 (2001).
[12] I. V. Kozhevnikov, S. Holmes, M. R. H. Siddiqui, Appl. Catal. A: General, **214**, 47 (2001).
[13] V. Sasca, M. Stefanescu, A. Popa, J. Thermal. Anal. Cal. **56,** 569 (1999).
[14] V. Sasca, M. Stefanescu, A. Popa, J. Therm. Anal. Cal. **72**, 311 (2003).
[15] A. Popa, V. Sasca, S. Crisan, M. Stefanescu, Ann. West Univ. Timişoara, ser. Chem. **9**(1), 85 (2000).
[16] A. Popa, B. Puşcaşu, V. Sasca, V. Mazur, Ann. West Univ. Timişoara Ser. Chem. **9**(1), 95 (2000).
[17] A. Popa, V. Sasca, R. Marinkovic-Neducin, E. E. Kis, Rev. Roum. Chim. in press.
[18] A. Popa, V. Sasca, M. Stefănescu, E. E. Kis, R. Marinkovic-Neducin, J. Serb. Chem. Soc. in press.